

The Oxidation Mechanism of Aniline by Ozone Water and Ozone Micro-nano Bubble Water and Its Influencing Factors

Zeming Xie

Zhejiang Gongshang University

Jiali Shentu

Zhejiang Gongshang University

Yuyang Long

Zhejiang Gongshang University

Li Lu

Zhejiang Gongshang University

Dongsheng Shen

Zhejiang Gongshang University

Shengqi Qi (✉ qishengqi@zjgsu.edu.cn)

Zhejiang Gongshang University

Research Article

Keywords: aniline, ozone micro-nano bubble water, oxidation, pH, ion, pathway

Posted Date: January 10th, 2022

DOI: <https://doi.org/10.21203/rs.3.rs-1137097/v1>

License: © ⓘ This work is licensed under a Creative Commons Attribution 4.0 International License.

[Read Full License](#)

The oxidation mechanism of aniline by ozone water and ozone micro-nano bubble water and its influencing factors

Zeming Xie¹, Jiali Shentu^{1,2}, Yuyang Long^{1,2}, Li Lu^{1,2}, Dongsheng Shen^{1,2*}, Shengqi Qi^{1,2*}

1 Zhejiang Provincial Key Laboratory of Solid Waste Treatment and Recycling, Zhejiang Gongshang University, Hangzhou 310012, PR China

2 Instrumental Analysis Center of Zhejiang Gongshang University, Hangzhou 310012, PR China

*Corresponding author

Abstract

Aniline is a kind of refractory contaminant that is difficult to be degraded by microorganisms. Ozone is a green and efficient reagent to oxidize aniline, while the ozone oxidation efficiency is restricted by the low ozone mass transfer rate. Micro-nano bubble ozonation has been developed as a new method to significantly improve the ozone utilization rate, while the characteristics of ozone micro-nano bubble when compared with dissolved ozone is not clear. The paper carried out batch experiments to research the oxidation effect of aniline by ozone water (OW) and ozone micro-nano bubble water (OMNBW), and found that the degradation rate of aniline by OMNBW was 2.8~5.9% higher than that by OW. The increase of pH had a negative effect on the degradation of aniline by OW and OMNBW. SO_4^{2-} , Cl^- , HCO_3^- and Mg^{2+} could inhibit the degradation efficiency by 0.04%, 0.99%, 0.44% and 10.4% for OW, while the ratios were 1.1%, 6.4%, 4.1% and 1.5% for OMNBW. The addition of humic acid and fulvic acid could decrease the oxidation rate of aniline by 35% and 49% for OW, while the ratios were 41% and 62% for OMNBW. Through quenching experiment, it was found that the direct oxidation by ozone molecules and the indirect oxidation by superoxide radicals were main pathways for aniline oxidation by OW and OMNBW. This work provided a practical guide for the application of OMNBW in wastewater and groundwater treatment process.

Keywords: aniline, ozone micro-nano bubble water, oxidation, pH, ion, pathway

30 **1. Introduction**

31 Aniline is an important chemical material and widely used in dyes, pesticides,
32 explosive materials, pharmaceuticals and other industries (Huang et al. 2017, Zhou et
33 al. 2014). Aniline is used to synthesize pesticides, chemical brighteners, dyes, etc. It is
34 also a common by-product of petroleum, papermaking and coal industry (Zabihi-
35 Mobarakeh and Nezamzadeh-Ejhieh 2015). Aniline is mutagenic, teratogenic and
36 carcinogenic, and has been listed as one of 129 priority-controlled pollutants by the U.S.
37 Environmental Protection Agency (USEPA) (Trautwein et al. 2015). In addition, aniline
38 is difficult to degrade and easy to maintain high toxicity even at low concentrations
39 (Orge et al. 2017). Therefore, it is necessary to develop water treatment technologies to
40 degrade aniline in order to meet the relative standards.

41 The remediation technology of polluted water included physical adsorption,
42 biological process and chemical oxidation. However, for wastewater containing
43 complex components, the efficiency of physical adsorption was very limited (Liu et al.
44 2009). For relatively persistent pollutants such as aniline, biological methods were
45 inefficient and usually spent more time than chemical methods (Ikehata et al. 2008).
46 Chemical oxidation was one of the most commonly used methods for water treatment
47 by different reagents, such as Fenton reagent, potassium permanganate, persulfate and
48 ozone. However, the oxidation efficiency of Fenton process was highly dependent on
49 pH and was easily affected by the various substances in actual water, such as chloride
50 and bicarbonate (Neyens and Baeyens 2003). In addition, hydrogen peroxide was
51 unstable with a short half-life (Clarizia et al. 2017). Persulfate must be activated before
52 it could be used for water treatment, but both catalyst and sulfate would produce a large
53 number of by-products, resulting in secondary pollution (Hou et al. 2012). Chemical
54 oxidation by permanganate would produce MnO_2 , which might also lead to secondary
55 pollution (Li and Schwartz 2005).

56 Compared with other treatment technologies, ozone had been widely applied in

57 the treatment of drinking water and reclaimed water (Miao et al. 2015, Shen et al. 2008),
58 because it produced fewer secondary pollutants than other oxidants. When ozone was
59 applied to oxidize contaminants in water, ozone gas was often injected directly by gas
60 sparger at the designed place. In this situation, the oxidation effect could only be
61 significant in its impact radius, which was near the injection point (Mccray and Falta
62 1996, Yao et al. 2020). Some studies combine ozone with surfactants to extend the
63 impact range, such as sodium dodecyl benzene sulfonate (Kim et al. 2004), while the
64 addition of surfactants would also cause secondary pollution.

65 Bubbles with a diameter between 200 nm and 10 μm are usually called micro-nano
66 bubbles (MNBs) (Agarwal et al. 2011). MNBs solutions might be a feasible option for
67 the continuous introduction of gaseous oxidizing agents to contaminated water. Ozone
68 micro-nano bubble water (OMNBW) was formed by the release of pressurized
69 ozonated water. Compared with water containing ozone (OW), the small radius of
70 MNBs made it more stable in water (Shangguan et al. 2018). In addition, MNBs had
71 large specific surface area and high interior gas pressure, which was related to the high
72 mass transfer rate of ozone from the gas phase to the liquid phase as well as the high
73 gas dissolution capability (Ikeura et al. 2011, Li et al. 2013, Takahashi et al. 2015).
74 When MNBs shrunk in water, charged ions quickly concentrated and enriched on a very
75 narrow bubble interface, so MNBs had higher zeta potential (Takahashi et al. 2007).
76 MNBs also had stronger migration ability, which had the potential ability to overcome
77 the heterogeneity in porous media (Choi et al. 2008). OMNBW had been proven to be
78 an effective oxidant for the oxidation of various organic pollutants, such as polycyclic
79 aromatic hydrocarbons, chlorinated hydrocarbons and dyes (Hu and Xia 2018, Zhang
80 et al. 2019). However, the oxidation mechanism of OMNBW and the influence of raw
81 water quality was still not clear, which impeded the application of OMNBW in practical
82 engineering.

83 This paper compared the oxidation efficiency and pathway of aniline by OMNBW
84 and OW, since the formation of MNBs in this study was through the release of
85 pressurized water. The effect of different water quality conditions, such as aniline

86 concentration, pH, inorganic ions and dissolved organic matter (DOM), were all studied
87 in this paper. In addition, the oxidation mechanisms of aniline by OW and OMNBW
88 were analyzed through quenching experiment. This paper could help guide the
89 application of OMNBW in wastewater and groundwater treatment engineering.

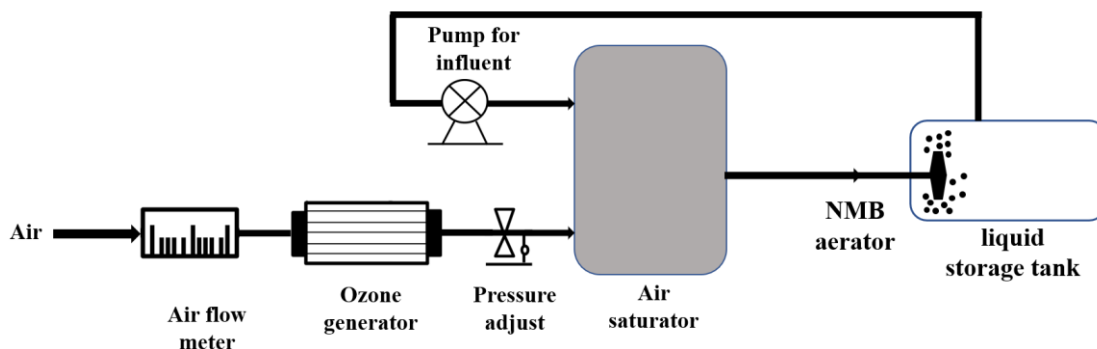
90 **2. Materials and methods**

91 **2.1 Chemicals and reagents**

92 The chemicals used in the experiment, sodium sulfate (purity $\geq 99\%$), sodium
93 chloride (purity $\geq 99.5\%$), sodium thiosulfate ($\text{Na}_2\text{S}_2\text{O}_3$) (purity $\geq 97\%$) were of
94 analytical grade supplied by Shanghai Lingfeng Chemical Reagent Co. Ltd.
95 Magnesium sulphate (purity $\geq 99\%$) was of analytical grade supplied by Xilong
96 Scientific Co. Ltd. Tert-butyl alcohol (TBA) (purity $\geq 99\%$) was of analytical grade
97 supplied by China National Pharmaceutical Group Co. Ltd. Sodium bicarbonate
98 (purity $\geq 99\%$), indigo disulfonate (purity $\geq 99\%$), *p*-benzoquinone (*p*-BQ) (purity \geq
99 98%), fulvic acid (FA, purity $\geq 85\%$), furfuryl alcohol (purity $\geq 98\%$), humic acid (HA,
100 purity $\geq 90\%$) were of analytical grade supplied by Shanghai Macklin Biochemical Co.
101 Ltd.

102 **2.2 Production of OMNBW and OW**

103 OMNBW was created by a continuous OMNBW generation apparatus (HG-WNF-
104 1, Hangzhou Guiguan Company, China). Ozone was generated from air in the ozone
105 generator. As shown in Fig. 1, the simulated tap water and the air containing ozone were
106 fed into the saturator at the flow rate of 360 mL/min and 140 mL/min, respectively. The
107 ozonized water was pressurized to 300 kPa in the air saturator, and it was then released
108 into the liquid storage tank with the volume of 12.5 L through the release head. The
109 water in the liquid storage tank was controlled at 10 °C through ice bath. Stable
110 dissolved ozone concentration at 1.36 mg/L could be obtained by aerating for about 5
111 min in the liquid storage tank.



112
113 **Fig. 1. Schematic diagram of OMNBW generation apparatus**

114 OW was produced by bubbling air containing ozone into water in a cylinder with
115 its volume of 1 L through a microporous diffuser, in which ozonized air was produced
116 by an ozone generator (FL-803A, China). Ice was also added in water before aeration
117 to control its temperature at 10 °C. The aeration process kept for about 3 min to reach
118 the stable ozone concentration at 1.36 mg/L.

119 **2.3 Aniline oxidation experiment**

120 When the aniline oxidation experiment by OMNBW and OW was carried out, 140
121 mL aniline solution with the temperature of 10 °C and a rotator were added in a conical
122 flask of 280 mL before the addition of OMNBW, and the conical flask was placed on a
123 magnetic stirrer with the rotating speed of 200 rpm. 140 mL OMNBW or OW were
124 scooped from the liquid storage tank or cylinder and quickly poured into the conical
125 flask. Then the flask was quickly sealed by the rubber stopper. The rubber stopper had
126 two holes, in which one hole was connected with a syringe with its volume of 100 mL
127 to balance the pressure, and the other hole was connected with the sampling port. 10
128 mL water in the flask was sampled each time by gastight syringe at various time
129 intervals up to 5 min. The obtained water sample was quenched by adding 1 mL
130 Na₂S₂O₃ solution with its concentration of 0.1 M, and then it was filtered by the 0.22
131 μm membrane for detection.

132 The influence of pH on the degradation of aniline by ozonation was investigated
133 by adding H₂SO₄ or NaOH solution with its concentration of 0.01 M to adjust pH
134 between 5.0 and 9.0. When the effect of ions was considered, 250 mg/L SO₄²⁻

135 (Na₂SO₄), 200 mg/L HCO₃⁻ (NaHCO₃), 250 mg/L Cl⁻ (NaCl) or 450 mg/L Mg²⁺
136 (MgSO₄) was mixed with aniline solution individually before the oxidation process.
137 When the effect of dissolved organic matter was considered, humic acid (HA) or fulvic
138 acid (FA) with its concentration of 50 mg/L was added to the aniline solution. The
139 mixed solution was stirred evenly by the magnetic stirrer before the oxidation
140 experiment.

141 In the quenching experiments, sodium thiosulfate, TBA or *p*-BQ was first mixed
142 with aniline solution individually, and the mixed solution was stirred evenly. The
143 molar ratios of sodium thiosulfate, TBA and *p*-BQ to aniline were 1330:1, 1256:1 and
144 860:1 respectively in order to completely quench the objective reaction. The
145 decomposition kinetics of ozone in OMNBW and OW were also carried out in this
146 paper. In this experiment, OMNBW or OW with its volume of 280 mL was added
147 directly into the same conical flask, and then the solution was sampled by gastight
148 syringe at various time intervals up to 40 min. Unless specified, all experiments were
149 carried out when the initial aniline concentration was 1 mg/L, temperature was 10 °C,
150 pH was 8.0 and stirring speed was 200 rpm. All experiments were conducted in
151 duplicate.

152 **2.4 Analytical methods**

153 The ozone concentration of OMNBW and OW was monitored using the indigo
154 method (Wang et al. 2019). Briefly, 1 mL indigo solution with its concentration of 1.25
155 mM and 10 mL sample solution was mixed in a glass colorimetric tube. The absorption
156 measurements for the indigo method were performed at the wavelength of 610 nm on
157 a spectrophotometer (SG1000, China).

158 The aniline concentration was measured by high performance liquid
159 chromatography (HPLC) (Waters e2695, USA) with a C18 column (4.6×150 mm, 5
160 μm). The mobile phase was an aqueous mixture (40% methanol and 60% water) at a
161 flow rate of 1 mL/min. The injection volume was 10 μL, and the liquid sample was
162 measured at the wavelength of 233 nm.

3. Results and discussion

3.1 The kinetics of ozone self-decomposition

The pseudo first-order kinetic model could be used to show the difference of self-decomposition rate between OMNBW and OW as Eq. (1).

$$\frac{dC}{dt} = -k_1 C \quad (1)$$

where C was the dissolved ozone concentration (mg/L), k_1 was the first-order decomposition coefficient (s^{-1}), t was the reaction time (s). Eq. (1) could be integrated to obtain the following equation:

$$\ln \frac{C_t}{C_0} = -k_1 t \quad (2)$$

where C_t was the dissolved ozone concentration at time t (mg/L), C_0 was the initial dissolved ozone concentration (mg/L). The decomposition of ozone in OMNBW and OW systems was shown in Fig. 2.

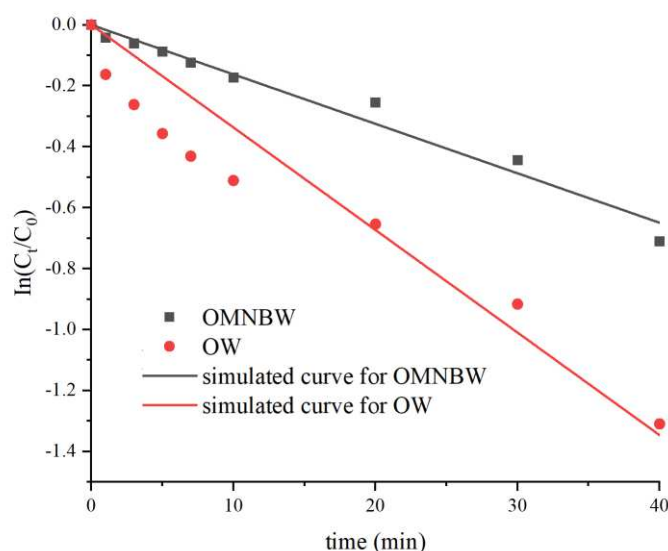


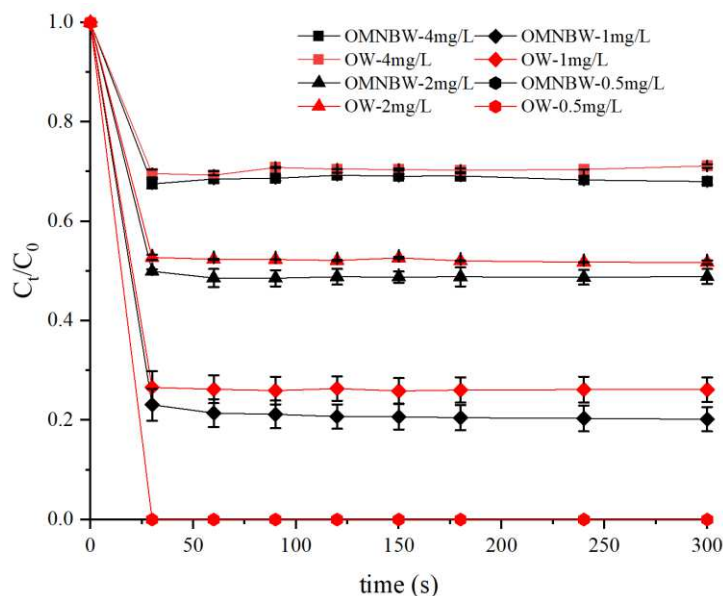
Fig. 2. Ozone self-decomposition curve in OMNBW and OW

The k_1 value for OMNBW and OW were 0.016 min^{-1} and 0.033 min^{-1} respectively, which showed that the self-decomposition of ozone in OMNBW was much slower than that in OW. Previous studies showed that the half-life of ozone in the gas phase was about twice longer than that in the liquid phase (Derco et al. 2021). When pressurized

181 water containing ozone was released into the tank, a large fraction of ozone in OMNBW
 182 still existed in the gas phase, and then gradually dissolved in water with the
 183 disappearance of bubbles (Fujioka et al. 2021), which led to a longer half-life of ozone
 184 in OMNBW. The slow release of ozone from gas phase to the liquid phase induced a
 185 slower but longer reaction rate between ozone and target contaminants.

186 3.2 The aniline oxidation kinetics by OMNBW and OW

187 The reaction of ozone and organic substance in aqueous media could be described
 188 by the direct molecular reaction by ozone molecules and indirect reaction by hydroxyl
 189 radicals ($\bullet\text{OH}$) (Hamdi El Najjar et al. 2013). Fig. 3 showed that both OMNBW and
 190 OW could oxidize aniline within 30 s, which could be deemed as an instantaneous
 191 reaction. Turhan and Uzman (2010) found that when aniline was oxidized by ozone in
 192 a bubble column, it was completely degraded within 30 min. Aeration by air bubbles
 193 containing ozone required the accumulation of ozone in water, while the direct
 194 oxidation by OW could obtain a very high ozone concentration at the start of reaction,
 195 which led to the instantaneous degradation of aniline within 30 s in this study.



196
 197 **Fig. 3. Degradation of aniline by OW and OMNBW with different initial aniline**
 198 **concentrations**

199 When the initial aniline concentration was 0.5 mg/L, aniline was completely

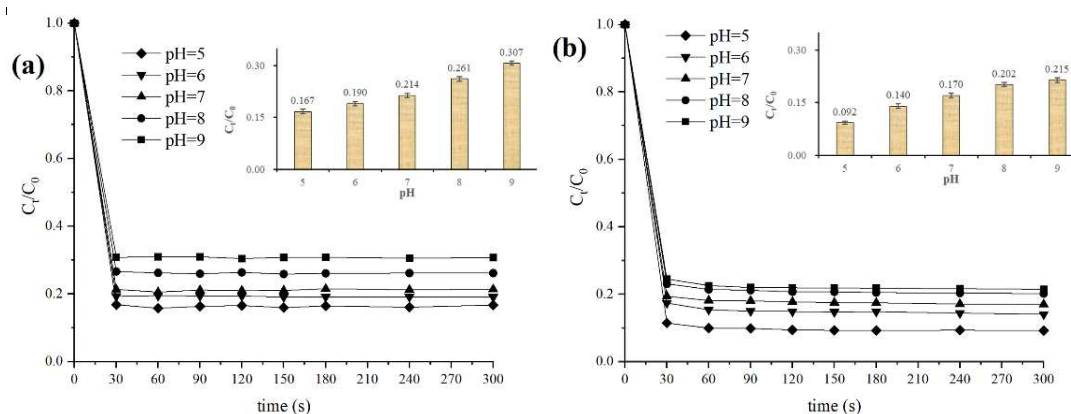
200 degraded within 30 s by both OMNBW and OW. When the initial aniline concentration
201 was 1 mg/L, the degradation rate of aniline by OMNBW reached 79.8% in 5 min, which
202 was 5.9% higher than that by OW. When the initial aniline concentrations were 2 mg/L
203 and 4 mg/L, the degradation rate by OMNBW were 51.1% and 32%, which were 2.8%
204 and 3.1% higher than that by OW respectively. The results showed that although aniline
205 could react with ozone molecules directly, the removal rate of aniline by OMNBW was
206 still higher than that by OW when the dissolved ozone concentration was the same.
207 Previous studies showed that MNBs would release a large amount of •OH in the process
208 of annihilation (Liu et al. 2016). At the same time, MNBs had small size and large
209 specific surface area (Agarwal et al. 2011). Therefore, MNBs could adsorb more
210 contaminants and increase the oxidation rate, which finally induced a higher removal
211 rate of aniline in this study.

212 **3.3 Influence of pH**

213 It could be observed from Fig. 4 that the degradation rate of aniline by OMNBW
214 or OW both decreased significantly with the increase of pH. Theoretically, during the
215 oxidation process of organic substances by ozone, alkaline conditions would be
216 beneficial to the degradation of contaminants than acidic conditions, because alkaline
217 environment would produce more •OH that would oxidize contaminants without
218 selectivity (Remucal et al. 2020). In addition, a higher pH would also increase the
219 lifetime of MNBs, because MNBs became more negative and had stronger repulsive
220 force (Hamamoto et al. 2018). However, the higher pH during ozonation would also
221 lead to the instability of ozone molecules (Derco et al. 2021), which further resulted in
222 the quick decrease of aqueous ozone concentration.

223 In alkaline environment, molecular ozone would easily decompose to •OH, which
224 had a very short survival time with the half-life of 10^{-3} μ s (Mei et al. 2019). If it did
225 not contact pollutants for the first time, •OH would die out and may reduce the ozone
226 utilization rate. Therefore, the aniline oxidation rate by OW decreased from 83.3% to
227 69.3% when pH increased from 5 to 9. However, MNBs would produce much •OH in

228 the process of annihilation (Liu et al. 2016), which could degrade aniline effectively. In
 229 addition, the surface of MNBs were negative charged, and MNBs had small size and
 230 large specific surface area (Agarwal et al. 2011), which could effectively adsorb
 231 pollutants. Therefore, the degradation rate of aniline by OMNBW when pH was 9 was
 232 only 1.3% lower than that when pH was 8 (Fig. 4b), which indicated that the oxidation
 233 of aniline by OMNBW was less affected by the solution pH when compared with OW.



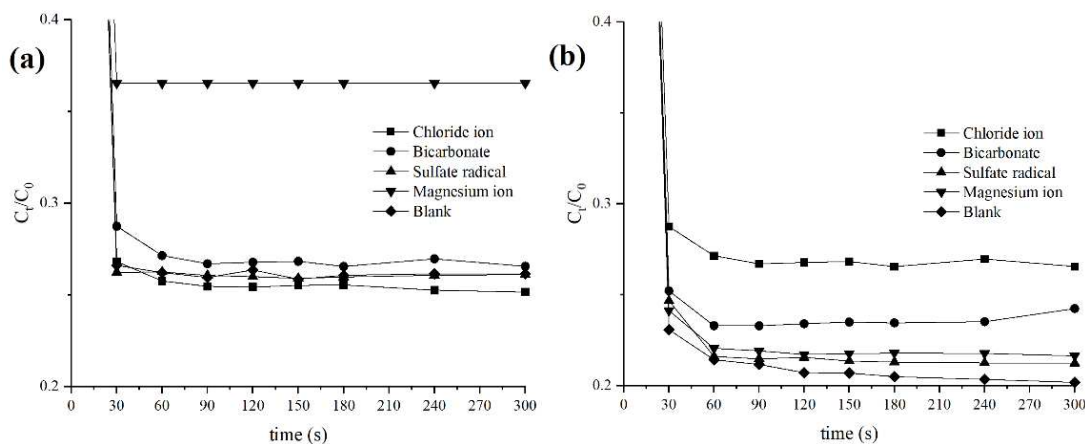
234
 235 **Fig. 4. Influence of pH on aniline degradation (a: OW; b: OMNBW)**

236 3.4 Influence of inorganic ions

237 Different anions had different influence on ozone oxidation effect (Ji et al. 2018).
 238 In this paper, the influence of common ions on the degradation of aniline by OMNBW
 239 and OW was investigated, which included SO_4^{2-} , Cl^- , HCO_3^- and Mg^{2+} that were
 240 representative ions in the raw water (Santafé-Moros and Gozávez-Zafrilla 2010). As
 241 shown in Fig. 5a, SO_4^{2-} , Cl^- and HCO_3^- only reduced the degradation efficiency by
 242 0.04%, 0.99% and 0.42% respectively for OW, which was related to the direct oxidation
 243 of aniline by molecular ozone. For OMNBW, SO_4^{2-} inhibited the degradation rate of
 244 aniline by 1.1%, but Cl^- and HCO_3^- inhibited the degradation rate by 6.4% and 4.1%
 245 respectively, which showed that these three anions had a relatively significant influence
 246 on the oxidation of aniline by OMNBW. According to previous studies, HCO_3^- and Cl^-
 247 were well-known free radical inhibitors and had been widely used for $\bullet\text{OH}$ scavenging
 248 (Clarizia et al. 2017, Liu et al. 2013). Therefore, the inhibition of Cl^- and HCO_3^- on
 249 OMNBW might be through the inhibition of free radical pathway. However, OW did
 250 not form as much $\bullet\text{OH}$ as OMNBW (Liu et al. 2016), so the inhibition by HCO_3^- and

251 Cl^- were not significant for OW.

252 It could also be observed from Fig. 5 that Mg^{2+} inhibited the OW oxidation rate
253 by 10.4%, but it only inhibited the OMNBW oxidation rate by 1.5%. The effects of
254 Mg^{2+} on ozone oxidation pollutants were mainly divided into two aspects. Mg^{2+} could
255 promote the production of $\bullet\text{OH}$ and had complexation with some ozonation
256 intermediates such as carboxylic acids, so that these intermediates were easier to be
257 oxidized (Sui et al. 2010). In addition, Mg^{2+} could promote the decomposition of ozone
258 and inhibit the degradation efficiency of contaminant (Rischbieter et al. 2000, Sui et al.
259 2010), which was consistent with the aniline oxidation results by OW. However, Mg^{2+}
260 has less inhibition on aniline degradation efficiency by OMNBW. It might be caused
261 by the negatively charged bubbles that could preferentially adsorb Mg^{2+} (Agarwal et al.
262 2011), which reduced the catalytic effect of Mg^{2+} on dissolved ozone. In addition,
263 bubbles also inhibited the direct contact between gas-phase ozone and Mg^{2+} , which
264 prolonged the ozone lifetime at the same time.

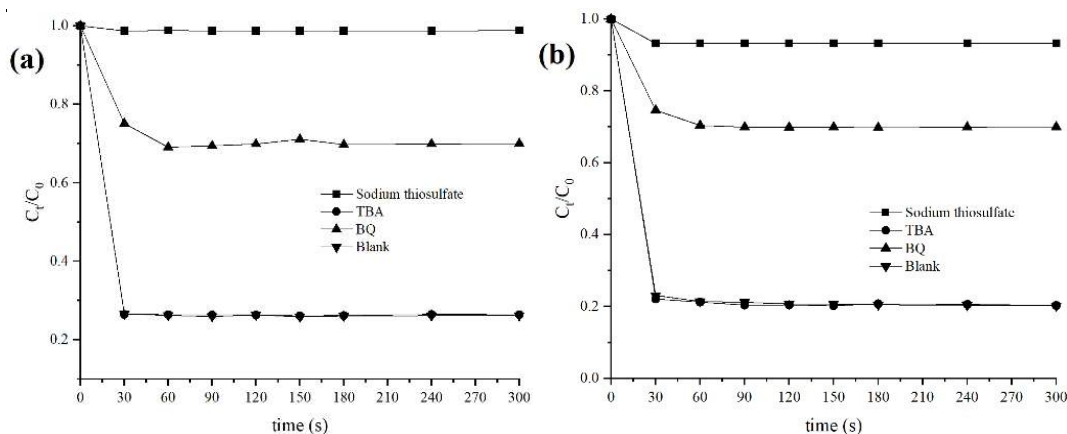


265
266 **Fig. 5. Influence of different ions on aniline oxidation (a: OW; b: OMNBW)**

267 3.5 Influence of DOM

268 The influence of HA and FA on aniline oxidation by OMNBW and OW was shown
269 in Fig. 6, which showed that both HA and FA had great inhibition effects on the
270 oxidation of aniline by OMNBW and OW. When HA was added in the solution, the
271 degradation rate of aniline by OW and OMNBW decreased by 35% and 41%, while FA
272 inhibited the aniline degradation rate by 49% and 62% respectively, indicating that FA

273 with small molecules would react with oxidants more easily (Wang et al. 2017).
 274 According to previous research, HA and FA could be oxidized by ozone, which
 275 competed with aniline and reduced the aniline oxidation rate as well (Wang et al. 2020).
 276 The ozone oxidation mechanism by OMNBW was mainly divided into the direct
 277 oxidation by molecular ozone dissolved in water and the "interface degradation" after
 278 pollutants were adsorbed on bubbles. DOM with a high concentration would be
 279 adsorbed by bubbles and covered the bubble surface, which competed for limited
 280 adsorption sites. Therefore, the existence of DOM would inhibit the oxidation of aniline
 281 by the competed adsorption and oxidation. It could be inferred that for OMNBW, the
 282 oxidation of contaminants was more relied on the molar concentration of contaminants
 283 rather than the chemical reaction rate. In OMNBW, contaminants were more easily
 284 degraded when they were adsorbed on bubble surface. Both the adsorption capacity of
 285 contaminants on bubble surface and the molar concentration of contaminants would
 286 affect the ozone oxidation rate, which improved the oxidation selectivity of ozone by
 287 OMNBW.

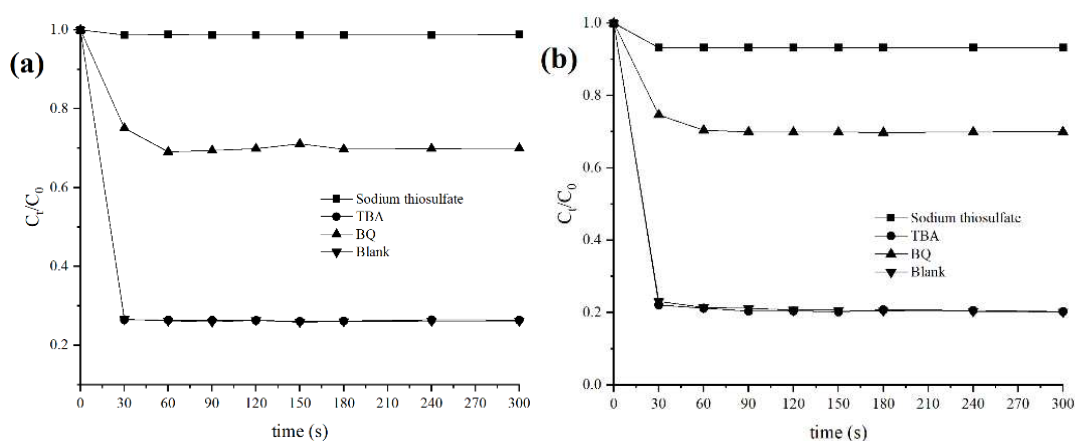


288
 289 **Fig. 6. Influence of DOM on aniline degradation (a: OW; b: OMNBW)**

290 3.6 The oxidation pathways by free radicals

291 Previous data in Section 3.2 showed that at the same dissolved ozone concentration,
 292 OMNBW had a stronger removal rate of aniline than OW, which might be caused by
 293 the free radicals that was formed in OMNBW. TBA was very easy to react with $\bullet\text{OH}$
 294 ($k_{\text{TBA}\cdot\text{OH}} = 6.0 \times 10^8 \text{ M}^{-1} \text{ s}^{-1}$), but it hardly reacted with ozone ($k_{\text{TBA}\cdot\text{O}_3} = 3.0 \times 10^{-3} \text{ M}^{-1} \text{ s}^{-1}$)

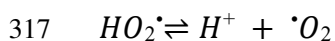
295 ¹⁾ (Nawrocki 2013, Nawrocki and Kasprzyk-Hordern 2010). Therefore, TBA was
 296 applied to identify the existence of •OH in OMNBW and OW. Fig. 7 showed that the
 297 aniline oxidation rate by OW only decreased by 0.30% after the addition of TBA as
 298 scavenger, while the oxidation rate by OMNBW only decreased by 0.15%. It indicated
 299 that indirect pathway by •OH took a very small fraction in the aniline oxidation process.
 300 In addition, previous studies reported that TBA tended to disperse in aqueous solution
 301 and was not efficient in capturing radicals near bubble surface (Yao et al. 2020).
 302 Therefore, the reason for the low quenching effect in OMNBW might be the generation
 303 of •OH at the bubble surface rather than in the solution.



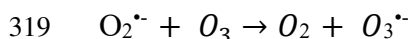
304
 305 **Fig. 7. Effect of free radical on aniline degradation (a: OW; b: OMNBW)**

306 Ozone could initiate free radical chain reactions in water (Acero and Gunten 2001,
 307 Staehelin and Hoigne 1985). These free radical chain reactions played an important role
 308 in promoting the decomposition of ozone into various reactive oxygen species (e.g. •
 309 OH, O₂⁻, O₃⁻) (Guo et al. 2021). Ozone could react with water or hydroxyl ion to
 310 produce some primary •OH and HO₂• (Eqs. 3, 4), and these radicals could further
 311 react to form O₂⁻ (Eq. 5). Once formed, O₂⁻ could quickly react with ozone to form
 312 O₃⁻ (Eqs. 6, 7). There were increasing studies claiming that O₂⁻ was the main reactive
 313 oxygen species (ROS) for the removal of ozone-resistant pollutants (Tan et al. 2017,
 314 Wang et al. 2016).

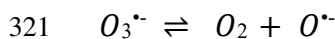




318 (5)



320 (6)



322 (7)

323 *p*-BQ was frequently used to trap superoxide radicals ($O_2^{\bullet -}$) with a rate constant
324 of $9.0\sim 9.8 \times 10^8 \text{ M}^{-1} \text{ s}^{-1}$ (Burns et al. 2012), and *p*-BQ could also react with $\bullet\text{OH}$ with
325 a rate constant of $1.2 \times 10^9 \text{ M}^{-1} \text{ s}^{-1}$ (Burns et al. 2012). However, *p*-BQ hardly reacted
326 with ozone ($k_{p\text{-BQ-O}_3} = 2.5 \times 10^3 \text{ M}^{-1} \text{ s}^{-1}$) (Mvula and von Sonntag 2003). As the quenching
327 experiment by TBA had proven that $\bullet\text{OH}$ could hardly play any role in the reaction,
328 the effect of *p*-BQ on the aniline oxidation could be attributed to the effect of $O_2^{\bullet -}$. Fig.
329 7 showed that the degradation of aniline by OW was inhibited by 44% after the addition
330 of *p*-BQ, while the inhibition rate increased to 50% for OMNBW, indicating that $O_2^{\bullet -}$
331 played important role in the aniline oxidation process. Compared with OW, OMNBW
332 produced more $O_2^{\bullet -}$, which indicates that OMNBW could trigger more chain reactions
333 in the degradation of aniline. In addition, when pH was neutral or alkaline, the indirect
334 oxidation by $O_2^{\bullet -}$ was the main oxidation pathway (Beltran et al. 1994, Derco et al.
335 2021).

336 $\text{Na}_2\text{S}_2\text{O}_3$ could react with almost all oxidizing substances quickly because of its
337 strong reducibility, so it was often used as an oxidant scavenger (Shen et al. 2008). Fig.
338 7 showed that the addition of excessive $\text{Na}_2\text{S}_2\text{O}_3$ almost eliminate the ability of OW to
339 oxidize aniline. However, OMNBW could still oxidize aniline by 7.5%. If it was in
340 homogeneous aqueous solution, excess $\text{Na}_2\text{S}_2\text{O}_3$ should be able to quickly remove all
341 oxidative substances, which contradicted with the experimental result in this study. The
342 probable reason might be that negatively charged $\text{S}_2\text{O}_3^{2-}$ could not be effectively
343 adsorbed by negatively charged micro-nano bubbles (Li et al. 2014). On the contrary,
344 bubbles could effectively adsorb positively charged aniline molecules, resulting in the

345 oxidation reaction of aniline by ozone at the bubble interface, which led to the aniline
346 oxidation process.

347 **4. Conclusion**

348 In this paper, batch experiments were carried out to research the influence factors
349 and oxidation mechanism of aniline oxidation by OW and OMNBW. Experimental
350 results showed that the half-life of ozone in OMNBW was 106% larger than that of OW,
351 which was caused by the prolonged life of ozone in the gas phase in OMNBW. A lower
352 pH value would induce a higher oxidation efficiency of aniline for both OW and
353 OMNBW, but the degradation efficiency of OMNBW reduced less than OW when pH
354 rose from 8 to 9. SO_4^{2-} , Cl^- and HCO_3^- with their concentrations at 5~10 mM had almost
355 no effect on OW, but they could reduce the oxidation rate by 1.1%, 6.4% and 4.1% for
356 OMNBW respectively. For OW and OMNBW, Mg^{2+} could inhibit the aniline oxidation
357 rate by 10.4% and 1.5%, respectively. For OW and OMNBW, the addition of HA could
358 decrease the removal rate of aniline by 35% and 41%, while the ratios were 49% and
359 62% for FA. When OW acted as the oxidant, hydroxyl radical, superoxide radical and
360 molecular ozone contributed 0.3%, 43.7% and 56.0% for aniline oxidation, while for
361 OMNBW these ratios were 0.2%, 49.8% and 50.0% respectively. The addition of
362 excessive sodium thiosulfate completely inhibited the oxidation of aniline by OW, but
363 aniline was still oxidized by 7.5% in the OMNBW system, indicating the interfacial
364 oxidation of aniline in bubble surface. This paper provided a strong support for the
365 application of OMNBW in wastewater and groundwater treatment engineering.

366

367 **Statements and Declarations**

368 **Funding**

369 This paper was supported by the National Natural Science Foundation of China
370 (No. 42107261), the Open Project Foundation from Zhejiang Key Laboratory of Urban
371 Environmental Processes and Pollution Control (No. NUEORS202001), and the
372 Program for the Introduction of Talents in Zhejiang Gongshang University (No.

373 1260XJ2120010, 1260XJ2320040).

374 **Ethical approval**

375 Not applicable

376 **Competing interests**

377 The authors have no relevant financial or non-financial interests to disclose.

378 **Consent to participate**

379 All participants agreed to participate in this study and signed the informed consents.

380 **Consent to publish**

381 All authors reviewed and approved the manuscript for publication.

382 **Author contributions**

383 ZX did the aniline oxidation experiment, and wrote the original draft of the paper.
384 JS, YL and LL all offered valuable suggestions for the manuscript. DS helped form the
385 experimental plan, guided the experiment, and offered valuable suggestions for the
386 manuscript. SQ guided the experiment, revised the manuscript and obtained funding
387 for the study.

388 **Data availability**

389 The datasets used and analyzed during the current study are available from the
390 corresponding author on reasonable request.

391

392 **References**

- 393 Acero JL, Gunten UV (2001) Characterization of oxidation processes: Ozonation and the AOP
394 O₃/H₂O₂. *J Am Water Works Ass* 93(10):90-100. <https://doi.org/10.1002/j.1551-8833.2001.tb09311.x>
395
396 Agarwal A, Ng WJ, Liu Y (2011) Principle and applications of microbubble and nanobubble
397 technology for water treatment. *Chemosphere* 84(9):1175-1180.
398 <https://doi.org/10.1016/j.chemosphere.2011.05.054>
399 Beltran FJ, García-Araya J, Acedo B (1994) Advanced oxidation of atrazine in water—I. Ozonation.
400 *Water Res* 28(10):2153-2164. [https://doi.org/10.1016/0043-1354\(94\)90027-2](https://doi.org/10.1016/0043-1354(94)90027-2)
401 Burns JM, Cooper WJ, Ferry JL, King DW, DiMento BP, McNeill K, Miller CJ, Miller WL, Peake

402 BM, Rusak SA, Rose AL, Waite TD (2012) Methods for reactive oxygen species (ROS)
403 detection in aqueous environments. *Aquat Sci* 74(4):683-734. [https://doi.org/10.1007/s00027-](https://doi.org/10.1007/s00027-012-0251-x)
404 [012-0251-x](https://doi.org/10.1007/s00027-012-0251-x)

405 Choi YJ, Park JY, Kim YJ, Nam K (2008) Flow characteristics of microbubble suspensions in porous
406 media as an oxygen carrier. *Clean-Soil Air Water* 36(1):59-65.
407 <https://doi.org/10.1002/clen.200700146>

408 Clarizia L, Russo D, Di Somma I, Marotta R, Andreozzi R (2017) Homogeneous photo-Fenton
409 processes at near neutral pH: A review. *Appl Catal B-Environ* 209:358-371.
410 <https://doi.org/10.1016/j.apcatb.2017.03.011>

411 Derco J, Gotvajn AŽ, Čižmárová O, Dudáš J, Sumegová L, Šimovičová K. (2021) Removal of
412 micropollutants by ozone-based processes. *Processes* 9(6):1013.
413 <https://doi.org/10.3390/pr9061013>

414 Fujioka S, Mizuno K, Terasaka K (2021) Dissolution and shrinking of a single microbubble in
415 stationary liquid with surfactants. *Chem Ing Tech* 93(1-2):216-222.
416 <https://doi.org/10.1002/cite.202000144>

417 Guo Y, Zhang Y, Yu G, Wang Y (2021) Revisiting the role of reactive oxygen species for pollutant
418 abatement during catalytic ozonation: The probe approach versus the scavenger approach. *Appl*
419 *Catal B-Environ* 280:119418. <https://doi.org/10.1016/j.apcatb.2020.119418>

420 Hamamoto S, Takemura T, Suzuki K, Nishimura T (2018) Effects of pH on nano-bubble stability
421 and transport in saturated porous media. *J Contam Hydrol* 208: 61-67.
422 <https://doi.org/10.1016/j.jconhyd.2017.12.001>

423 Hamdi El Najjar N, Touffet A, Deborde M, Journel R, Leitner NK (2013) Levofloxacin oxidation
424 by ozone and hydroxyl radicals: kinetic study, transformation products and toxicity.
425 *Chemosphere* 93(4):604-611. <https://doi.org/10.1016/j.chemosphere.2013.05.086>

426 Hou L, Zhang H, Xue X (2012) Ultrasound enhanced heterogeneous activation of peroxydisulfate
427 by magnetite catalyst for the degradation of tetracycline in water. *Sep Purif Technol* 84:147-
428 152. <https://doi.org/10.1016/j.seppur.2011.06.023>

429 Hu L, Xia Z (2018) Application of ozone micro-nano-bubbles to groundwater remediation. *J Hazard*
430 *Mater* 342:446-453. <https://doi.org/10.1016/j.jhazmat.2017.08.030>

431 Huang Q, Zhang J, He Z, Shi P, Qin X, Yao W (2017) Direct fabrication of lamellar self-supporting
432 Co₃O₄/N/C peroxymonosulfate activation catalysts for effective aniline degradation. *Chem*
433 *Eng J* 313:1088-1098. <https://doi.org/10.1016/j.cej.2016.11.002>

434 Ikehata K, Gamal El-Din M, Snyder SA (2008) Ozonation and advanced oxidation treatment of
435 emerging organic pollutants in water and wastewater. *Ozone-Sci Eng* 30(1):21-26.
436 <https://doi.org/10.1080/01919510701728970>

437 Ikeura H, Kobayashi F, Tamaki M (2011) Removal of residual pesticides in vegetables using ozone
438 microbubbles. *J Hazard Mater* 186(1):956-959. <https://doi.org/10.1016/j.jhazmat.2010.11.094>

439 Ji H, Gong Y, Duan J, Zhao D, Liu W (2018) Degradation of petroleum hydrocarbons in seawater
440 by simulated surface-level atmospheric ozone: Reaction kinetics and effect of oil dispersant.
441 *Mar Pollut Bull* 135:427-440. <https://doi.org/10.1016/j.marpolbul.2018.07.047>

442 Kim H, Soh HE., Annable MD, Kim DJ (2004) Surfactant-enhanced air sparging in saturated sand.
443 *Environ Sci Technol* 38(4):1170-1175. <https://doi.org/10.1021/es030547o>

-
- 444 Li H, Hu L, Song D, Al-Tabbaa A (2013) Subsurface transport behavior of micro-nano bubbles and
445 potential applications for groundwater remediation. *Int J Environ Res Public Health* 11(1):473-
446 486. <https://doi.org/10.3390/ijerph110100473>
- 447 Li H, Hu L, Song D, Lin F (2014) Characteristics of micro-nano bubbles and potential application
448 in groundwater bioremediation. *Water Environ Res* 86(9):844-851.
449 <https://doi.org/10.2175/106143014x14062131177953>
- 450 Li X, Schwartz F (2005) *Subsurface Contamination Remediation*, pp. 82-95.
451 <https://doi.org/10.1021/bk-2005-0904.ch004>
- 452 Liu S, Oshita S, Kawabata S, Makino Y, Yoshimoto T (2016) Identification of ROS produced by
453 nanobubbles and their positive and negative effects on vegetable seed germination. *Langmuir*
454 32(43):11295-11302. <https://doi.org/10.1021/acs.langmuir.6b01621>
- 455 Liu X, Zhang T, Zhou Y, Fang L, Shao Y (2013) Degradation of atenolol by UV/peroxymonosulfate:
456 kinetics, effect of operational parameters and mechanism. *Chemosphere* 93(11):2717-2724.
457 <https://doi.org/10.1016/j.chemosphere.2013.08.090>
- 458 Liu Z, Kanjo Y, Mizutani S (2009) Removal mechanisms for endocrine disrupting compounds
459 (EDCs) in wastewater treatment - physical means, biodegradation, and chemical advanced
460 oxidation: a review. *Sci Total Environ* 407(2):731-748.
461 <https://doi.org/10.1016/j.scitotenv.2008.08.039>
- 462 Mccray J, Falta R (1996) Defining the air sparging radius of influence for groundwater remediation.
463 *J Contam Hydrol* 24(1):25-52. [https://doi.org/10.1016/0169-7722\(96\)00005-8](https://doi.org/10.1016/0169-7722(96)00005-8)
- 464 Mei Q, Sun J, Han D, Wei B, An Z, Wang X, Xie J, Zhan J, He M (2019) Sulfate and hydroxyl
465 radicals-initiated degradation reaction on phenolic contaminants in the aqueous phase:
466 Mechanisms, kinetics and toxicity assessment. *Chem Eng J* 373:668-676.
467 <https://doi.org/10.1016/j.cej.2019.05.095>
- 468 Miao H, Cao M, Xu D, Ren H, Zhao M, Huang Z, Ruan W (2015) Degradation of phenazone in
469 aqueous solution with ozone: influencing factors and degradation pathways. *Chemosphere*
470 119:326-333. <https://doi.org/10.1016/j.chemosphere.2014.06.082>
- 471 Mvula E, von Sonntag C (2003) Ozonolysis of phenols in aqueous solution. *Org Biomol Chem*
472 1(10):1749-1756. <https://doi.org/10.1039/b301824p>
- 473 Nawrocki J (2013) Catalytic ozonation in water: Controversies and questions. Discussion paper.
474 *Appl Catal B-Environ* 142-143:465-471. <https://doi.org/10.1016/j.apcatb.2013.05.061>
- 475 Nawrocki J, Kasprzyk-Hordern B (2010) The efficiency and mechanisms of catalytic ozonation.
476 *Appl Catal B-Environ* 99(1-2):27-42. <https://doi.org/10.1016/j.apcatb.2010.06.033>
- 477 Neyens E, Baeyens J (2003) A review of classic Fenton's peroxidation as an advanced oxidation
478 technique. *J Hazard Mater* 98(1-3):33-50. [https://doi.org/10.1016/s0304-3894\(02\)00282-0](https://doi.org/10.1016/s0304-3894(02)00282-0)
- 479 Orge C, Faria J, Pereira MFR (2017) Photocatalytic ozonation of aniline with TiO₂-carbon
480 composite materials. *J Environ Manage* 195:208-215.
481 <https://doi.org/10.1016/j.jenvman.2016.07.091>
- 482 Remucal CK, Salhi E, Walpen N, von Gunten U (2020) Molecular-level transformation of dissolved
483 organic matter during oxidation by ozone and hydroxyl radical. *Environ Sci Technol*
484 54(16):10351-10360. <https://doi.org/10.1021/acs.est.0c03052>
- 485 Rischbieter E, Stein H, Schumpe A (2000) Ozone solubilities in water and aqueous salt solutions. *J*

486 Chem Eng Data 45(2):338-340. <https://doi.org/10.1021/je990263c>

487 Santafé-Moros A, Gozálviz-Zafrilla JM (2010) Nanofiltration study of the interaction between
488 bicarbonate and nitrate ions. *Desalination* 250(2):773-777.
489 <https://doi.org/10.1016/j.desal.2008.11.039>

490 Shangguan Y, Yu S, Gong C, Wang Y, Yang W, Hou L (2018) A review of microbubble and its
491 applications in ozonation. *Iop Conference: Earth and Environmental Science* 128:012149.
492 <https://doi.org/10.1088/1755-1315/128/1/012149>

493 Shen J, Chen Z, Xu Z, Li X, Xu B, Qi F (2008) Kinetics and mechanism of degradation of p-
494 chloronitrobenzene in water by ozonation. *J Hazard Mater* 152(3):1325-1331.
495 <https://doi.org/10.1016/j.jhazmat.2007.08.009>

496 Staehelin J, Hoigne J (1985) Decomposition of ozone in water in the presence of organic solutes
497 acting as promoters and inhibitors of radical chain reactions. *Environ Sci Technol* 19(12):1206-
498 1213. <https://doi.org/10.1021/es00142a012>

499 Sui M, Sheng L, Ma J, Tian F, Lu K (2010) Assistance of magnesium cations on degradation of
500 refractory organic pollutant by ozone: Nitrobenzene as model compound. *Ozone-Sci Eng*
501 32(2):113-121. <https://doi.org/10.1080/01919510903579460>

502 Takahashi M, Chiba K, Li P (2007) Free-radical generation from collapsing microbubbles in the
503 absence of a dynamic stimulus. *J Phys Chem B* 111(6):1343-1347.
504 <https://doi.org/10.1021/jp0669254>

505 Takahashi M, Horibe H, Matsuura K, Tatera K (2015) Effect of microbubbles on ozonized water for
506 photoresist removal. *J Photopolym Sci Tec* 28(2):293-298.
507 <https://doi.org/10.2494/photopolymer.28.293>

508 Tan X, Wan Y, Huang Y, He C, Zhang Z, He Z, Hu L, Zeng J, Shu D (2017) Three-dimensional
509 MnO₂ porous hollow microspheres for enhanced activity as ozonation catalysts in degradation
510 of bisphenol A. *J Hazard Mater* 321:162-172. <https://doi.org/10.1016/j.jhazmat.2016.09.013>

511 Trautwein G, El Bakkali B, Alcañiz-Monge J, Artetxe B, Reinoso S, Gutiérrez-Zorrilla JM (2015)
512 Dimeric assemblies of lanthanide-stabilised dilacunary Keggin tungstogermanates: A new
513 class of catalysts for the selective oxidation of aniline. *J Catal* 331:110-117.
514 <https://doi.org/10.1016/j.jcat.2015.09.004>

515 Turhan K, Uzman S (2010) The degradation products of aniline in the solutions with ozone and
516 kinetic investigations. *Annali Di Chimica* 97(10):1129-1138.
517 <https://doi.org/10.1002/adic.200790096>

518 Wang Y, Xie Y, Sun H, Xiao J, Cao H, Wang S (2016) Hierarchical shape-controlled mixed-valence
519 calcium manganites for catalytic ozonation of aqueous phenolic compounds. *Catal Sci Technol*.
520 6(9): 2918-2929. <https://doi.org/10.1039/c5cy01967b>

521 Wang F, Huang Y, Zhuo X, He C, Li Q (2020) Molecular-level transformation characteristics of
522 refractory organics in landfill leachate during ozonation treatment. *Sci Total Environ*
523 749:141558. <https://doi.org/10.1016/j.scitotenv.2020.141558>

524 Wang H, Wang Y, Lou Z, Zhu N, Yuan H (2017) The degradation processes of refractory substances
525 in nanofiltration concentrated leachate using micro-ozonation. *Waste Manage* 69:274-280.
526 <https://doi.org/10.1016/j.wasman.2017.08.048>

527 Wang J, Quan X, Chen S, Yu H, Liu G (2019) Enhanced catalytic ozonation by highly dispersed

528 CeO₂ on carbon nanotubes for mineralization of organic pollutants. *J Hazard Mater* 368:621-
529 629. <https://doi.org/10.1016/j.jhazmat.2019.01.095>

530 Yao J, Yu Y, Qu R, Chen J, Huo Z, Zhu F, Wang Z (2020) Fe-activated peroxymonosulfate enhances
531 the degradation of dibutyl phthalate on ground quartz sand. *Environ Sci Technol* 54(14):9052-
532 9061. <https://doi.org/10.1021/acs.est.0c00793>

533 Zabihi-Mobarakeh H, Nezamzadeh-Ejhi A (2015) Application of supported TiO₂ onto Iranian
534 clinoptilolite nanoparticles in the photodegradation of mixture of aniline and 2, 4-dinitroaniline
535 aqueous solution. *J Ind Eng Chem* 26:315-321. <https://doi.org/10.1016/j.jiec.2014.12.003>

536 Zhang M, Feng Y, Zhang D, Dong L, Pan X (2019) Ozone-encapsulated colloidal gas aphrons for
537 in situ and targeting remediation of phenanthrene-contaminated sediment-aquifer. *Water Res*
538 160:29-38. <https://doi.org/10.1016/j.watres.2019.05.043>

539 Zhou Y, Gu X, Zhang R, Lu J (2014) Removal of aniline from aqueous solution using pine sawdust
540 modified with citric acid and β -cyclodextrin. *Ind Eng Chem Res* 53(2):887-894.
541 <https://doi.org/10.1021/ie403829s>

542